PERGAMON

Solid State Communications 112 (1999) 471–476

solid state communications

www.elsevier.com/locate/ssc

Solid solution formation in the new cuprate system $(Sr, K)_{1-x}(Ca, Na)_xCuO_{2\pm z}$ $(0 \leq x \leq 0.5)$

E. Chavira*, E. Hernández, O. Navarro, L. Baños, J. Guzmán

Instituto de Investigaciones en Materiales, UNAM Apartado Postal 70-360, 04510 México D.F., Mexico

Received 28 April 1999; accepted 29 June 1999 by R.C. Dynes

Abstract

Synthesis and some experimental results of the new cuprate system $(Sr, K)_{1-x}(Ca, Na)_xCuO_{2\pm z}(0.0 \leq x \leq 1.0)$ are reported for the first time. We prepared a series of polycrystalline samples of this system with *x*-steps of 0.1, by solid-state reaction method in air at ambient pressure below melt temperature. It is observed the formation of a solid solution in the range $0 \leq x \leq 0.5$ at 750°C. The characterization of the samples by X-ray powder diffraction indicates that the single phase is isostructural to the one for Cu_2SrO_3 compound, reported in the JCPDS-International Center for Diffraction Data (ICDD) file No. 39-0250, which has an orthorhombic unit cell. The compositions in the range $0.6 \leq x \leq 1.0$ have an unknown phase and *CuO*. Further characterization studies by scanning electron microscopy, thermogravimetric and differential thermal analysis are shown.

Keywords: B. Chemical synthesis; C. Scanning and transmission electron microscopy; D. Thermodynamic properties; E. X-ray and γ-ray spectroscopies

1. Introduction

Since the discovery of the superconducting phenomena exhibited in ceramic materials with high-T_c, by J.G. Bednorz and K.A. Müller in l986 [1], intensive investigations has clarified important features, such as the *d*-wave symmetry in the superconducting gap [2], the singlet pairing between holes (instead of electrons) [3], and their short coherence length [4], in spite of no general consensus on the high-T_c superconducting mechanism. Furthermore, extensive studies have been devoted to design new materials by different synthetic routes and to understand how their structural features relate to their superconducting properties. However, this structure-properties relationship is clear only in some oxide ceramic compounds because of their phase stability.

The basic structure of the superconducting oxides can be described as intergrowths of $Cu-O_2$ planes with intervening slabs stacked along the *c*-axis. The cuprates can therefore be classified by the composition of the intervening slabs. Certain cuprates, however, have more complex structures consisting of structural units of different kinds of copper planes. For instance, it can be mention the following compounds Ln−123 [5,6], (Y, Pr)−124 [7–9] or Y−247 [10,11]. It is also well established, that in the cuprates superconductors the $Cu-O_2$ planes are an essential parte to describe the superconductivity mechanism in the high-T_c ceramic materials.

Searching for a complex cuprate in the Sr–Cu–O system [12], important efforts have been done. In 1992 Kinoshita and Yamada reported the synthesis of the $(Ba_{0.55}Sr_{0.45})_2Cu_{1.1}O_{2.2+\delta}(CO_3)_{0.9}$ system by hot isostatic pressing under 250 bar [13]. Uehara et al. succeeded in the preparation under high pressure of the structures with higher members of the $(CO_3)Sr_2Ca_{n-1}Cu_nO_{2n}$ to achieve superconductivity at 115 K for the third member [14]. Hiroi et al. showed that the substitution of Na for Ca was crucial for the appearance of superconductivity in $Ca_{2-x}Na_xCuO_2Cl_2$ [15]. Likewise, Kazakov et al. studied the $Sr_{2-x}M_xCuO_2CO_3$ system, M = Na or K, using a high pressure technique [16].

We report herein the synthesis and characterization of the new cuprate system $(Sr, K)_{1-x}(Ca, Na)_xCuO_{2\pm z}$ $(0 \leq x \leq 1)$, obtaining the formation of a solid solution with the

* Corresponding author.

0038-1098/99/$ - see front matter
PII: S0038-1098(99)00307-5

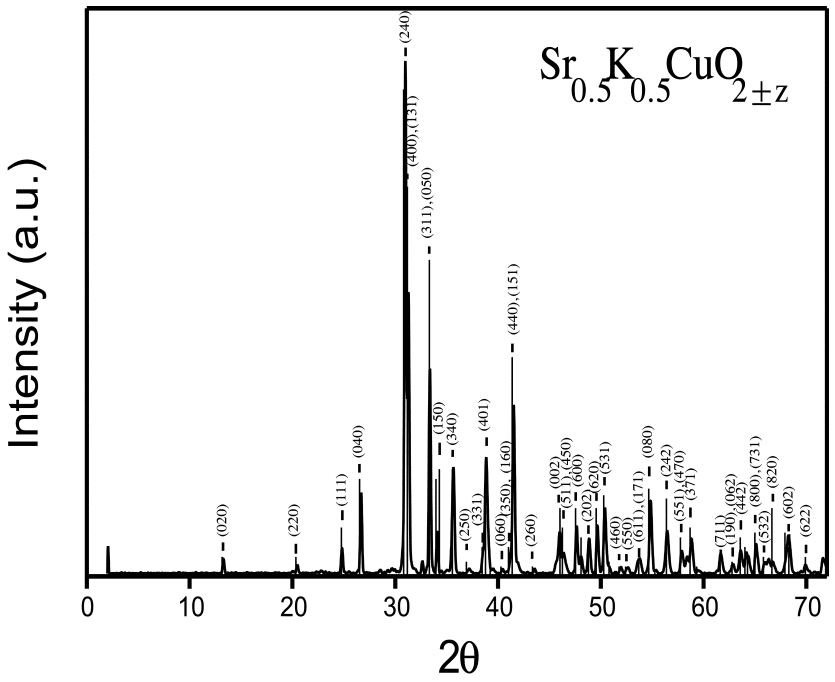

Fig. 1. X-ray powder pattern of $Sr_{0.5}K_{0.5}CuO_{2\pm z}$ composition overlapped with that of Cu_2SrO_3 compound.

solubility range ($0 \leq x \leq 0.5$), reproducible in terms of stoichiometry and crystalline structure.

2. Experimental procedure

2.1. Sample preparation

Polycrystalline samples of $(Sr, K)_{1-x}(Ca, Na)_xCuO_{2\pm z}$, ($0 \leq x \leq 1$) with steps of 0.1, were prepared by solid-state reaction. The started materials were $SrCO_3$ (Strem, 99%), $CaCO_3$ (CERAC, 99.95%), K_2CO_3 (CERAC, 99.999%), Na_2CO_3 (CERAC, 99.9%) and CuO (Aldrich, 99.99%), combined in stoichiometric proportions. Prior to weighting $SrCO_3, CaCO_3$ and Na_2CO_3 were preheating 20–25 min. at 100°C for dehydrated. The proper amount of K_2CO_3 was weighed in an Ar flowing glove bag to avoid contamination and decomposition of this reagent. The purity of all materials was verify by powder X-ray diffraction (XRD).

The started materials were mixed with an agate mortar and deposited in a high-density alumina crucibles. We observed by scanning electron microscopy (SEM) that the high-density alumina crucibles contaminate the samples, so we change the container material by Au foils. The decomposition of the oxysalts was done "in situ" for 16 h at a temperature between 630°C and 720°C (depending of the composition). The samples were weighing and analyzed by XRD in order to determine if the CO_2 was present. After the heat treatment for 16 h, the temperature in the samples was increasing gradually by steps of 10°C to follows the solid-state reaction and, in this way, determine the reaction temperature for each composition. The samples were slow cooled and analyzed by XRD to verify the completed reaction at each step of the temperature, we continue increasing the temperature till find a single phase.

2.2. Instrumentation

Samples were examined by powder X-ray diffraction, differential scanning calorimetry (DSC), thermogravimetric analysis (TGA), differential thermal analysis (DTA), scanning electron microscopy (SEM) and electron probe microanalysis (EDX). X-ray diffraction patterns were registered at room temperature on a SIEMENS D5000 diffractometer, equipped with an Ni-filtered, Cu$k_{\alpha 1}$ radiation, a graphite monochromator on the counter site and auto-divergence-slit system. This equipment is able to detect up to a minimum of 1% of impurities. The data were collected with a step-scan procedure in the range $2\theta = 2-70°$ with steps size of 0.01° and 0.02° and step time of 0.3 s. To calculate the lattice parameters we used a step size of 0.005° and a step time of 1.2 s. The lattices parameters were determined from the patterns using the least-squares method.

To study the possible phase transitions of the system we have done thermogravimetric analysis and differential thermal analysis using a TA Instruments 2910, with $\Delta T = \pm 0.001$°C. The instrument was calibrated against standard reference samples. In each measurement, we employed approximately 2 mg of the sample and the data were registered in air at ambient pressure. The morphology

Table 1
X-ray powder diffraction data of the $Sr_{0.5}K_{0.5}CuO_{2\pm z}$ composition

$d_{obs.}$(Å)	*hkl*	I/I_0	$d_{obs.}$(Å)	*hkl*	I/I_0	$d_{obs.}$(Å)	*hkl*	I/I_0
6.6571	020	8.60	2.1728	440,151	40.48	1.6286	242	19.69
4.3344	220	10.39	2.0755	260	13.10	1.5922	551,470	16.65
3.5826	111	14.69	1.9709	002	19.42	1.5688	371	18.60
3.3374	040	24.74	1.9561	511,450	15.96	1.5030	711	16.08
2.8837	240	100	1.9072	600	20.75	1.4774	190,062	14.56
2.8566	400,131	60.36	1.8908	170,022	15.66	1.4615	442	16.81
2.6831	311,050	46.96	1.8624	202	18.57	1.4507	660	16.73
2.6277	150	19.31	1.8344	620	20.87	1.4464	480,651	16.01
2.5151	340	29.39	1.8094	531	23.53	1.4319	800,731	18.19
2.4130	250	12.66	1.7593	460	13.74	1.4152	532	14.83
2.3340	331	16.01	1.7367	550	13.60	1.4007	820	14.89
2.3161	401	31.22	1.7026	611,171	15.14	1.3729	602	19.01
2.2291	060	13.08	1.6727	080	24.97	1.3444	622	14.24

and the elements content in the grains of the products were examined by a scanning electron microscopy (Leica-Cambridge Stereoscan 440), equipped with an Oxford/Link System electron probe microanalyser (EPMA). The SEM was operated in the analytical mode with a probe current of ≈211−324 pA, accelerated voltage of 20 kV, a QBSD detector and a counting time of 100 s.

3. Results and discussion

We obtained a single phase in the system $(Sr,K)_{1-x}(Ca,Na)_xCuO_{2\pm z}$ for $0 \le x \le 0.5$, in air and at ambient pressure. The reaction temperature were the following: for $0 \le x \le 0.3$ it was of 750°C during 19 h and for $0.4 \le x \le 0.5$ it was of 760°C during 30 h. For *x*-values between $0.6 \le x \le 1.0$ we had multiphases. Analyzing the XRD pattern of the $Sr_{0.5}K_{0.5}CuO_{2\pm z}$ composition it was observed that the single phase is isostructural to the one for Cu_2SrO_3 compound, which has an orthorhombic cell. In Fig. 1, we show the spectrum of the $Sr_{0.5}K_{0.5}CuO_{2\pm z}$ composition which is compared with the one reported by Klockow Eysel in JCPDS-ICDD file No. 39-0250. It can be noted that the lines of the $Sr_{0.5}K_{0.5}CuO_{2\pm z}$ diffractogram are

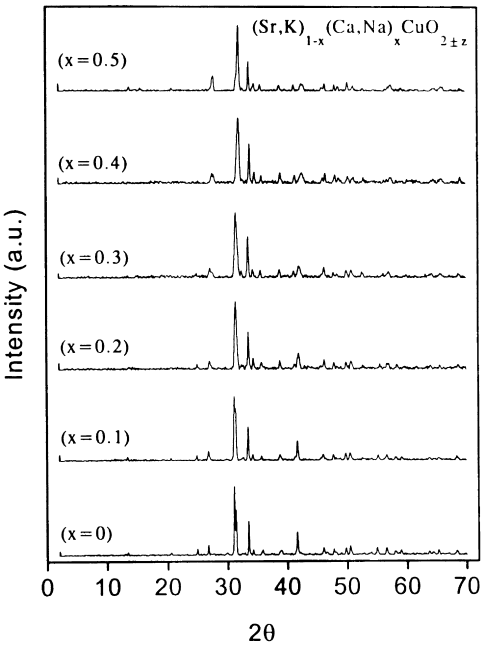

Fig. 2. Powder XRD diffractograms for $(Sr,K)_{1-x}(Ca,Na)_xCuO_{2\pm z}$ system with $x = 0, 0.1, 0.2, 0.3, 0.4$ and 0.5.

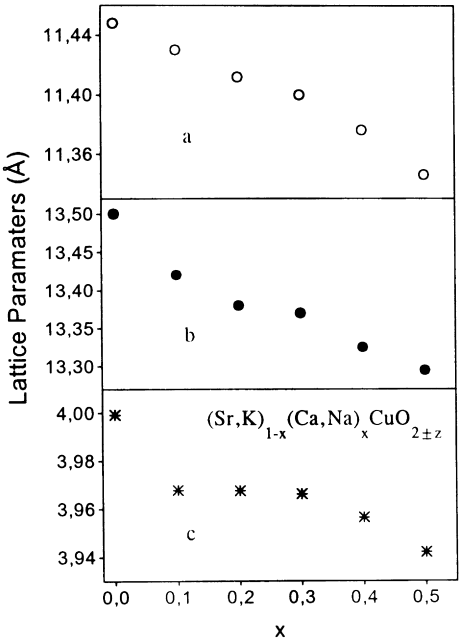

Fig. 3. Variation of the a-, b- and c-lattices parameters of $(Sr,K)_{1-x}(Ca,Na)_xCuO_{2\pm z}$ system.

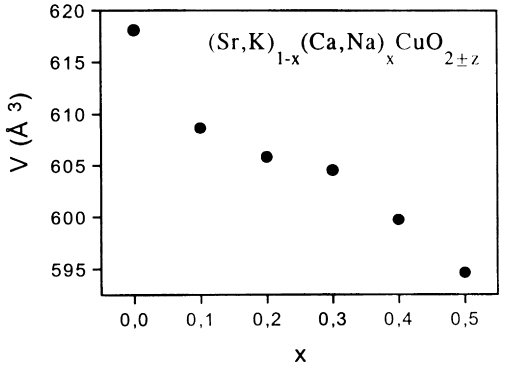

Fig. 4. Change of the unit cell volume as a function of concentration.

shifted to high angles (2θ), due to the substitution of different cations in the crystalline structure. The corresponding powder data are given in Table 1, the pattern was indexed on the basis of an orthorhombic unit cell. It is shown a series of diffractograms corresponding to the solid solution for the ollowing composition: $x = 0$ $Sr_{0.5}K_{0.5}CuO_{2\pm z}$, $x =$ 0.1 $(Sr_{0.45}K_{0.45})$ $(Ca_{0.05}Na_{0.05})$ $CuO_{2\pm z}$, $x = 0.2$ $(Sr_{0.40}K_{0.40})$ $(Ca_{0.1}Na_{0.1})$ $CuO_{2\pm z}$, $x =$ 0.3 $(Sr_{0.35}K_{0.35})$ $(Ca_{0.15}Na_{0.15})$ $CuO_{2\pm z}$, $x =$ 0.4 $(Sr_{0.30}K_{0.30})$ $(Ca_{0.20}Na_{0.20})$ $CuO_{2\pm z}$, $x =$ 0.5 $(Sr_{0.25}K_{0.25})(Ca_{0.25}Na_{0.25})CuO_{2\pm z}$.

In Fig. 2, it is observed that all the peaks have a shift on 2θ, due to the substitution of K, Ca and Na cations. The shift is exhibited in the changes of the unit cell parameters with

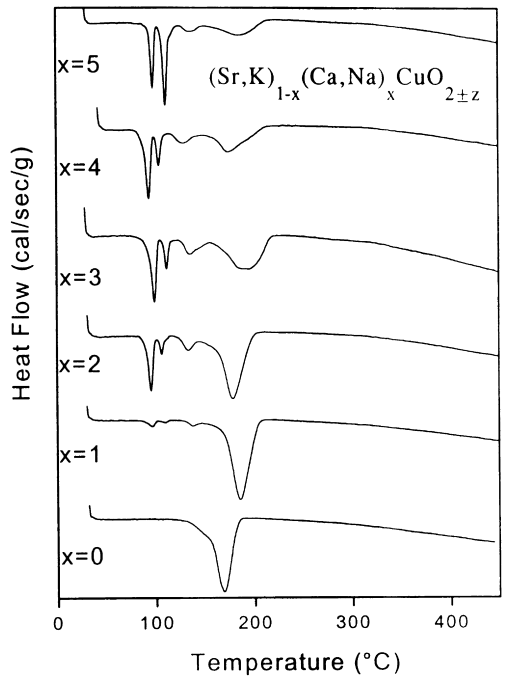

Fig. 5. Differential scanning calorimetry curves in air at 5°C/min from $x = 0.0$ to 0.5.

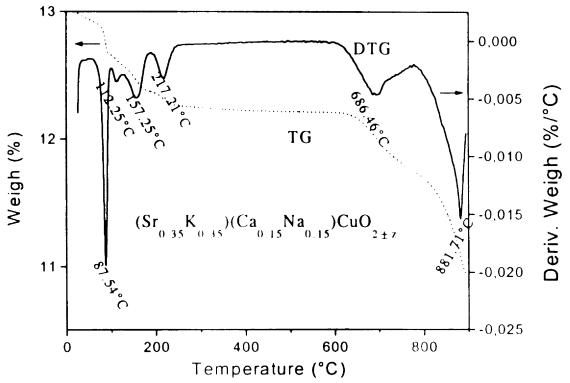

Fig. 6. Thermogravimetric analysis and its derivative for a concentration of $x = 0.3$ in air at 10°C/min.

the composition that govern the relative sizes of the active ions in the solid solution mechanism.

In order to obtain the lattice parameters of the solid solution, the polycrystal material was dropping in a standard sieve (400 mesh) to have the same particle size. The lattice parameters shown in Fig. 3, were calculated using the *d* values of (600), (050) and (002) reflections for the orthorhombic phase. The *a*-, *b*- and *c*-axis length decreases with increasing *x* values due to the smaller radius of Ca^{2+} and Na^{+} as compared to Sr^{2+} and K^{+}. Actually, SEM-EDX analyses indicate that the Sr^{2+} and K^{+} concentration of grains decrease with *x*. The behavior of the volume as a function of the concentration *x* in the solid-solution formation is shown in Fig. 4. The volume of the non-metallic $(Sr,K)_{1-x}(Ca,Na)_xCuO_{2\pm z}(0 \le x \le 0.2)$ system shows a negative departure from linearity. Negative departure from Vegard's Law in non-metallic systems may be evidence of a cationic order–disorder, this comportment could be also associated with the (400) peak in Fig. 2. For $x = 0.3-0.5$ we have a linear behavior which is in good agreement with Vegard's Law. This law is not really a law but rather is a generalization that applies to solid solutions formed by

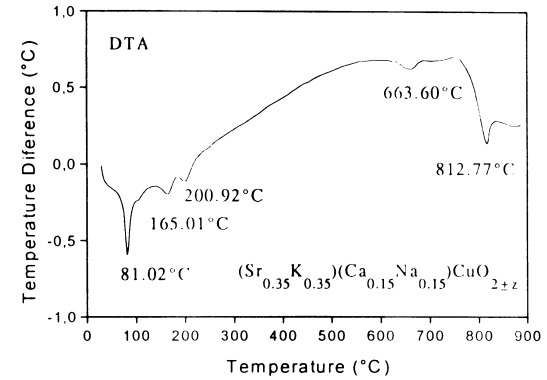

Fig. 7. Differential thermal analysis data of $(Sr_{0.35}K_{0.35})$ $(Ca_{0.15}Na_{0.15})CuO_{2\pm z}$ composition in air at 10°C/ min.

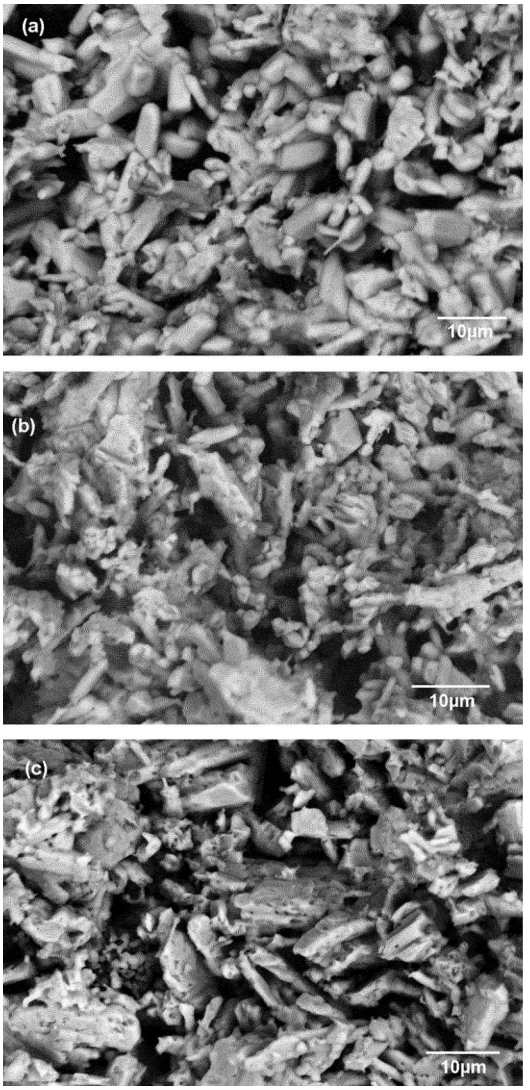

Fig. 8. Scanning electron micrographs of (a) $(Sr_{0.45}K_{0.45})(Ca_{0.05}Na_{0.05})CuO_{2\pm z}$, (b) $(Sr_{0.35}K_{0.35})(Ca_{0.15}Na_{0.15})CuO_{2\pm z}$ and (c) $(Sr_{0.25}K_{0.25})(Ca_{0.25}Na_{0.25})CuO_{2\pm z}$.

random substitution or distribution of ions [17], as in our case.

The thermal behavior of the reagents mixture is given in Figs. 5–7, where the curves of DSC ($x = 0.0-0.5$), TGA ($x = 0.3$) and DTA ($x = 0.3$) are shown. It can be observed the loss of water molecules between 25°C and 266°C of the oxysalts (Fig. 5), and the resulting changes of weight in the $(Sr_{0.35}K_{0.35})(Ca_{0.15}Na_{0.15})CuO_{2\pm z}$ which corresponds to the dehydrated sample (Fig. 6). This dehydration is also shows up on DTA curve (Fig. 7) as an endothermic behavior. It is also observed in the DTA curve the endothermic changes between 600°C and 780°C, which corresponds to the decomposition of the oxysalts and the formation of the phase, but it

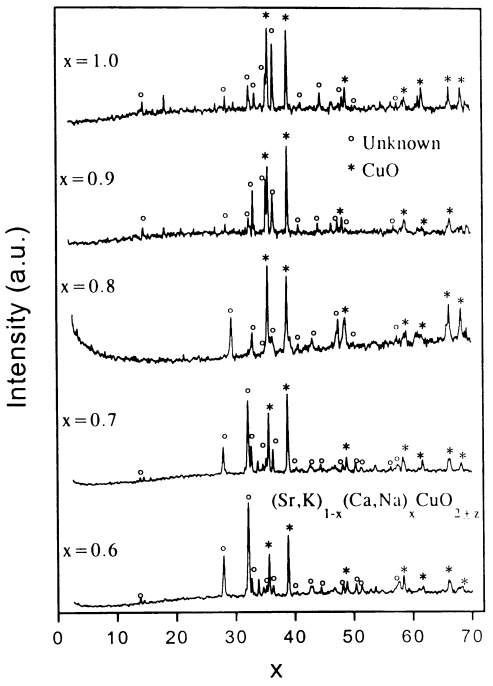

Fig. 9. X-ray diffraction patterns of $(Sr, K)_{1-x}(Ca, Na)_xCuO_{2\pm z}$ with $x = 0.6, 0.7, 0.8, 0.9$ and 1.0. The reflections of the unknown phase are indicated by open circles and the *CuO* by asterisks.

is difficult to assign to those individual peaks a definite chemical reactions. We do not have enough information to determined when the intermediate reaction took place, it means, the $(CO_3)^{-2}$ decomposition and the formation of the phase. It is common that some $(CO_3)^{-2}$ ions are trapped in the unit cell. Additionally, the last two broad steps after 600°C in Fig. 6, gives the weight loss associated with the $(CO_3)^{-2}$ decomposition and the melting phase.

The representative SEM micrographs of some concentrations are shown in Fig. 8, which were taken from sintering pellets. For $x = 0.1$ (Fig. 8a) the average particle size is on the order of 5 μm, for $x = 0.3$ (Fig. 8b) the sample shows that most of the grains size are in the range of 2−5 μm and for $x = 0.5$ the growth of the particles is like a cluster.

In Fig. 9, the powder XRD patterns are shown for the samples with starting compositions of $(Sr, K)_{1-x}(Ca, Na)_xCuO_{2\pm z}$ ($x = 0.6, 0.7, 0.8, 0.9$ and 1.0), most of diffraction peaks correspond to CuO and an unknown phase.

4. Conclusions

The $(Sr, K)_{1-x}(Ca, Na)_xCuO_{2\pm z}$ system for $0 \leq x \leq 1.0$ was prepared for the first time. It was determined the formation of the solid solution for the $(Sr, K)_{1-x}(Ca, Na)_xCuO_{2\pm z}$ system in the range of $0 \leq x \leq 0.5$, in air and at ambient

pressure which is a fast process. The structure of the solid solution is orthorhombic. To obtain the thermodynamic equilibrium of these compositions from a solid oxide mixture takes about 19–30 h at 750−760°C. The existence of the single phase in the above system was investigated by X-ray powder diffraction and scanning electron microscopy analysis.

Acknowledgements

This work was partially supported by grants from CONACyT 25582-E, DGAPA-UNAM IN109998 and TWAS 96-148 RG/CHE/LA. We also want to thanks to C. Vazquez for technical support.

References

[1] J.G. Bednorz, K.A. Müller, Z. Phys. B, 64 (1986) 189.
[2] D.A. Wollman, D.J. Van Harlingen, W.C. Lee, D.M. Ginsberg, A.J. Leggett, Phys. Rev. Lett., 71 (1998) 2134.
[3] E. Dagotto, Rev. Mod. Phys., 66 (1994) 763.
[4] R. Micnas, J. Ranninger, S. Robaszkiewicz, Rev. Mod. Phys., 62 (1990) 113.
[5] M.H. Wu, J.R. Aschburn, C.J. Tory, P.H. Hor, R.C. Meng, L. Gao, Z.H. Huang, Y.Q. Wang, C.W. Chu, Phys. Rev. Lett., 58 (1987) 908.
[6] M.B. Maple, Y. Dalichaough, G.M. Ferreira, R.R. Hake, B.W. Lee, J.J. Neumeier, M.S. Torikachvili, K.N. Yang, H. Zhou, Physica B, 148 (1987) 155.
[7] J.K. Liang, X.T. Xu, S.S. Xie, G.H. Rao, X.Y. Shao, Z.G. Duan, Z. Phys. B, 69 (1987) 137.
[8] L. Solderhelm, K. Zhang, D.G. Hinks, M.A. Beno, J.D. Jorgensen, C.U. Serge, I.K. Schuller, Nature 328 (1987) 6655.
[9] L-C. Tung, J.C. Chen, M.K. Wu, W. Guan, Phys. Rev. B, 59 (1999) 4504.
[10] P. Marsh, R.M. Fleming, M.L. Mandich, A.M. DeSantolo, L. Kwo, M. Hong, L.J. Martinez-Miranda, Nature, 234 (1988) 141.
[11] J. Karpinski, E. Kaldis, E. Jilek, S. Rusiecki, B. Bucher, Nature 336 (1988) 660.
[12] Z. Hiroi, M. Takano, M. Asuma, Y. Takeda, Nature 364 (1993) 315.
[13] K. Kinoshita, T. Yamada, Nature 357 (1992) 313.
[14] M. Uehara, M. Uoshima, S. Ishiyama, H. Nakata, J. Akimitsu, Y. Matsui, T. Arima, Y. Tokura, N. Mory, Physica C, 229 (1994) 310.
[15] Z. Hiroi, N. Kobayashi, M. Takano, Nature 371 (1994) 139.
[16] S.M. Kazakov, E.V. Antipov, C. Chaillout, J.J. Capponi, M. Brunner, J.L. Tholence, M. Marezio, Physica C, 253 (1995) 401.
[17] A.R. West, Solid State Chemistry and its Applications, John Wiley (1984).